Electronic Supplementary Material (ESI) for Chemical Science.

Supporting information for: Transition Voltages Respond to Synthetic Reorientation of Embedded Dipoles in Self-Assembled Monolayers

Andrii Kovalchuk,[†] Tarek Abu-Husein,[‡] Davide Fracasso,[†] David A. Egger,[¶,§] Egbert Zojer,[¶] Michael Zharnikov,[‖] Andreas Terfort,[‡] and Ryan C. Chiechi[*,†]

[†]*Stratingh Institute for Chemistry & Zernike Institute for Advanced Materials, University of Groningen, Nijenborgh 4, 9747 AG Groningen, The Netherlands*

[‡]*Institut für Anorganische und Analytische Chemie, Universität Frankfurt, Max-von-Laue-Straße 7, 60438 Frankfurt, Germany*

[¶]*Institute of Solid State Physics, NAWI Graz, Graz University of Technology, Graz, Austria*

[§]*Department of Materials and Interfaces, Weizmann Institute of Science, Rehovoth 76100, Israel*

[‖]*Angewandte Physikalische Chemie, Universität Heidelberg, Im Neuenheimer Feld 253, 69120 Heidelberg, Germany*

E-mail: r.c.chiechi@rug.nl

Contents

Experimental

Sample preparation

The Au substrates used in this work are made by mechanical Template Stripping (TS) as described elsewhere.[S1] In our case, we deposited 100 nm of Au (99.99%) by thermal vacuum deposition onto a 3" Silicon wafer (with no adhesion layer). Using UV-curable Optical Adhesive (OA) Norland 61, 1 cm^2 glass chips were glued on the metal surfaces. The TS procedure provides ultra flat smooth surfaces, which allows self-assembly process to achieve high yields of working junctions. All samples were made by incubation of freshly cleaved gold slides in 1 mM solutions in ethanol at room temperature for $\sim$ 24h. Prior to making a solution ethanol was degassed by bubbling nitrogen gas through for at least 20 minutes and all solutions were kept under nitrogen atmosphere to prevent undesirable oxidation of thiol anchoring group.

Data acqusition

Data were acquired in a home-built setup that is described in detail elsewhere.[S2] Samples were taken out from solution, carefully rinsed with pure ethanol and gently blown to dryness

with nitrogen. Each SAM was then measured by placing a sharp tip of EGaIn in visual contact with the surface and acquiring at least 1000 scans across 10 substrates for an average of ∼15 scans per junction. The traces in which the instrument reached compliance were considered short circuits and were discarded (they reflect only the compliance limit of the instrument and have no physical meaning). TP1-up showed lower solubility than both TP1 and TP1-down and showed signs of partial precipitation onto the gold surface leading to the appearance of traces where values of J were systematically *ca.* two of orders of magnitude lower than the geometric mean. These traces, which were present only in TP1-up data and made up a small fraction of the total traces, most likely reflect junctions comprising multilayers and were discarded. Histograms of the values of J at each value of V were then fit to Gaussian distributions. The standard deviation of a fit (σ) was then recalculated into 95% confidence interval using following equation CI = $t\frac{\sigma}{\sqrt{N}}$, where t is the coefficient in t-distribution and N is the number of degrees of freedom for our system ($N_{junctions} - 1$).

Table S1 shows statistics on junctions of SAMs of TP1, TP1-down and TP1-up. Each contact of EGaIn tip with the sample is considered a junction (total), junctions that worked without shorting—working, and junctions that worked but shorted during the measurements—shorted. "Total" yield of working junctions is calculated as a ratio of working over total number of junctions and "working" yield as a ratio of working-not-shorted over working.

Table S1: Statistics on junctions for SAMs of TP1, TP1-down and TP1-up. Last column showcases two ways of calculating the yield of working junctions.

SAM	Number of scans	Number of junctions total/working/shorted	Yield of working junctions total/working (%)
TP1	1320	95 / 43 / 0	45 / 100
TP1-down	1860	219 / 93 / 3	43 / 97
TP1-up	1170	126 / 94 / 3	75 / 97

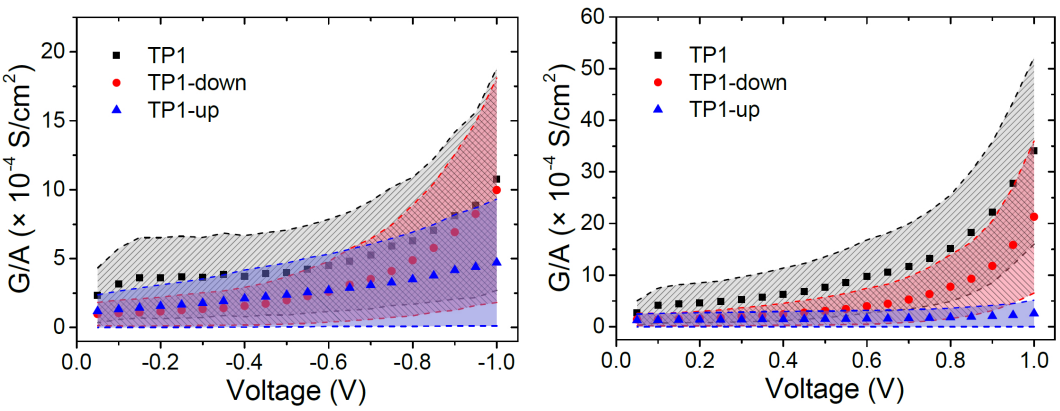

Figure S1: Conductance plots per unit of area for SAMs of TP1 (black squares), TP1-down (red circles) and TP1-up (blue triangles) for negative (on the left) and positive (on the right) bias. The 95% confidence bands are depicted as shaded areas. The three SAMs are indistinguishable at negative bias and only few data points of TP1-up differ from both TP1 and TP1-down at high positive bias.

Transition voltages

We calculate transition voltage by re-plotting each I/V trace in Fowler-Nordheim coordinates, $ln(I/V^2)$ versus $1/V$, and found the minimum from the numerical derivative. All values were then plotted in a histogram to which a Gaussian distribution was fit to get a peak value and a standard deviation (which is then recalculated into 95% CI as described above). We used Scientific Python to automate the entire process, providing only raw J/V data as an input. Figure S2 shows graphically how V_T relates to plots of $ln(I/V^2)$ versus $1/V$ and shows plots of $log|J|$ versus $|V|$ to highlight the opposite symmetry of TP1-up. The histograms for V_T along with Gaussian fits are presented in Figure S3.

In Figure S4 β- and V_T-analyses are presented for a series of alkanethiols (decanethiol, dodecanethiol and tetradecanethiol on Ag) and pyrimidine-containing series (TP1, TP1-up and TP1-down on Au). In case of alkanes, β-analysis is enough to conclude that current is dominated by molecules, not by interfaces or defects. However, in cases where J is not changing with d β-analysis is inapplicable, and a trend in V_T with $\Delta\Phi$ may be used analogously.

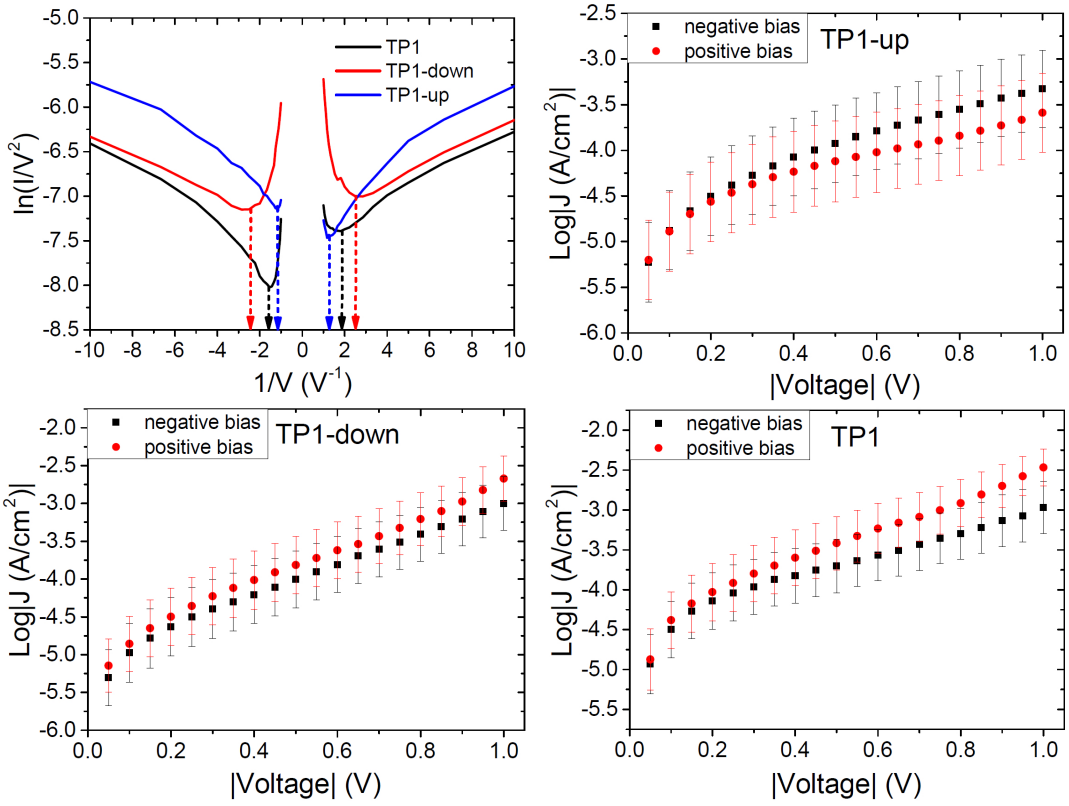

Figure S2: Fowler-Nordheim plot for selected $I(V)$ traces of SAMs of TP1, TP1-up and TP1-down (top left). Arrows indicate values, acquired after statistical analysis of all $I(V)$ data combined. Plots of Log$|J|$ vs $|V|$ for three SAMs, depicting slight asymmetry in $J(V)$ data. TP1 and TP1-down are more conductive under positive bias, while TP1-up—under negative bias.

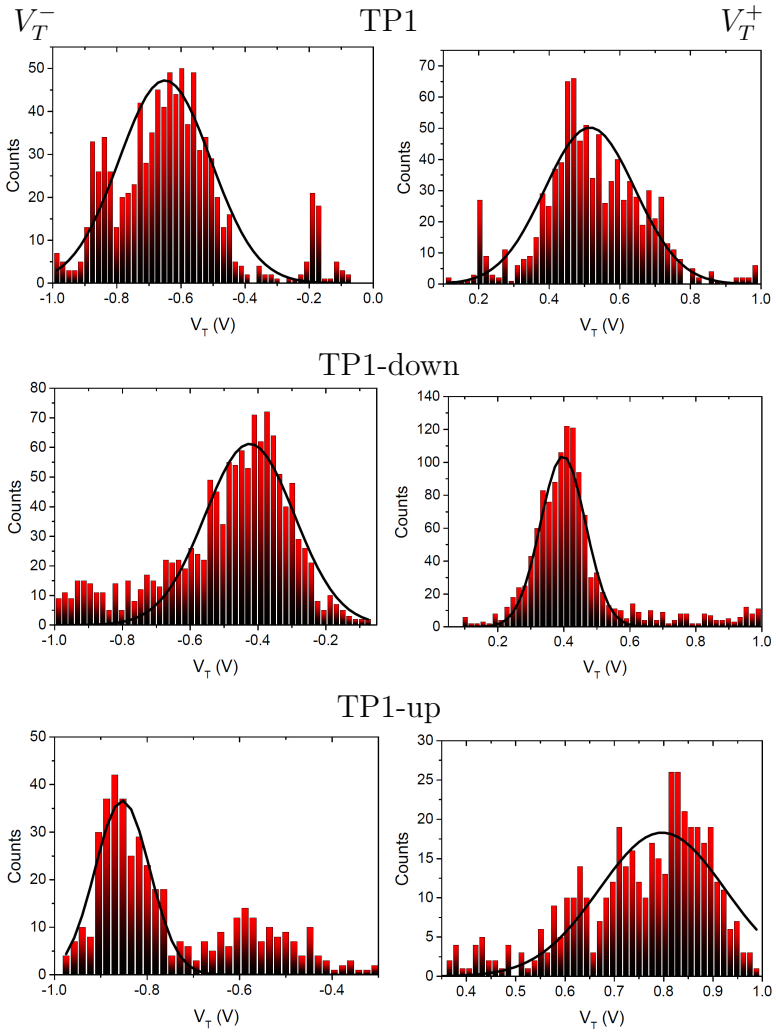

Figure S3: Histograms of V_T^- (left column) and V_T^+ (right column) along with Gaussian fits for SAMs of TP1, TP1-down and TP1-up.

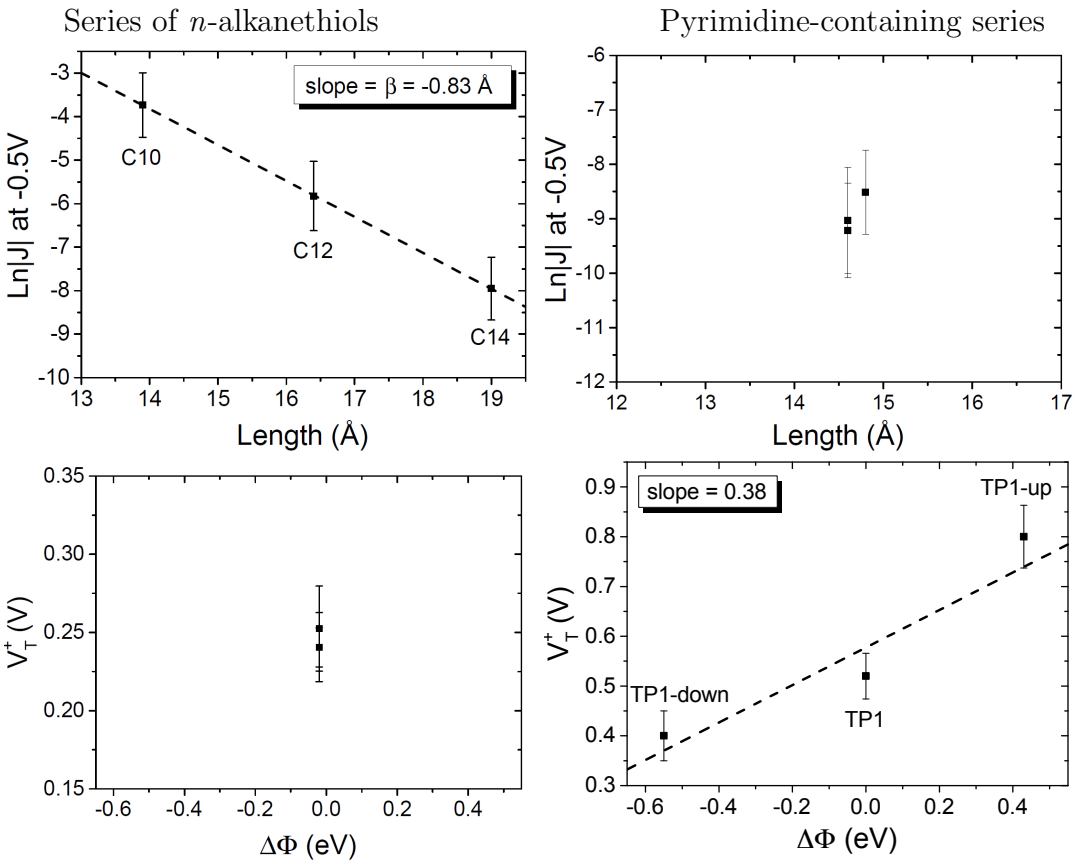

Figure S4: β-plots from Au^{TS}/SAM/EGaIn junctions for series of n-alkanethiols (decanethiol, dodecanethiol, and tetradecanethiol) and pyrimidine-containing series (TP1, TP1-down, and TP1-up)—top row. Plots of V_T vs WF shift for both series—bottom row, which show how a trend in V_T can be used as a molecular fingerprint (as an example data only of V_T^+ is presented for both series) similar to β for situations where d is invariant.

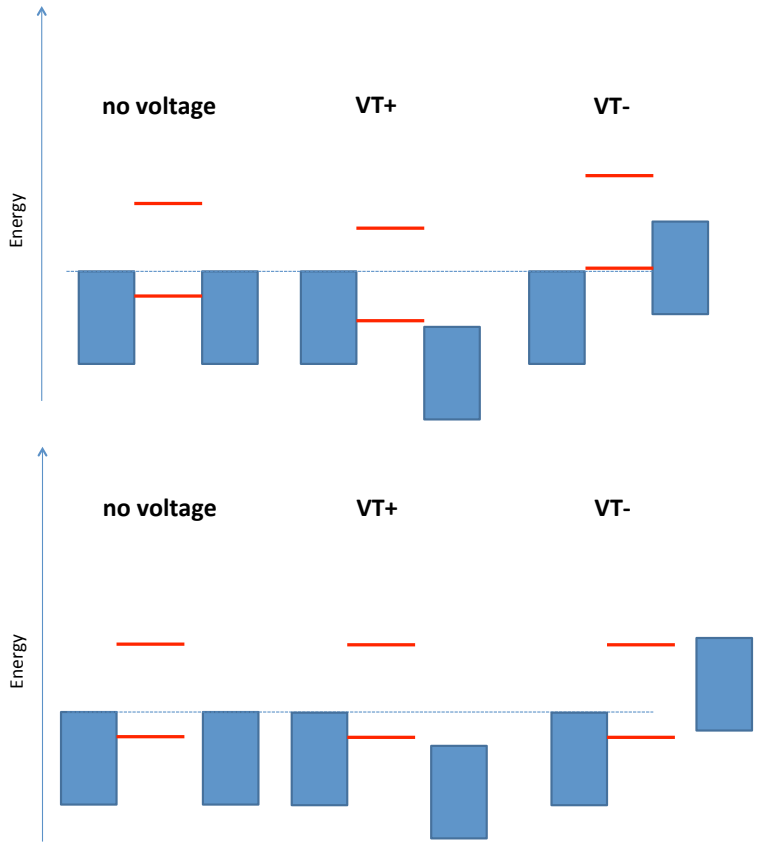

Figure S5: A schematic diagram of energy levels of a junction in two different limiting cases: (i) symmetric coupling, no tunneling gap (at the top) and (ii) asymmetric coupling, large tunneling gap (at the bottom). Dotted line represents chemical potential of the left electrode relative to which the voltage is applied. Case (i): half of the applied voltage drops between the molecule and the electrode on each side. This neglects that the molecular states are modified by the applied electric field. V_T^+ and V_T^- are expected to be identical. Case (ii): essentially all the voltage drops between the molecule and the second electrode leading to LUMO becoming available for electron transport. In this situation tunneling occurs through the HOMO, when applying a positive bias, and through the LUMO, when applying a negative bias. Consequently, $V_T^+ < V_T^-$ in situations when the HOMO is closer to E_f than the LUMO and, vice versa, $V_T^+ > V_T^-$ when the LUMO is closer.

Calculations

The substrate-SAM interfaces were modeled using a $(\sqrt{3}\times 3)$ surface unit cell containing two molecules in herringbone arrangement.[S3] The geometries of the SAMs were optimized using the VASP code[S4] applying the PBE functional[S5] and using the repeated-slab approach. The corresponding procedure is explained in detail in S3. Beyond what is described there, for calculating the electronic states in the SAMs considered here, we had to apply a hybrid functional (in the present case HSE06), to ensure a correct ordering of the electronic states bearing in mind the strongly differing self-interaction errors associated with *s*- and *p*-states and the high-lying occupied *s*-states in pyrimidines.[S6]

For the LUMO-derived states the opposite localization trend is observed in TP1-down and TP1-up SAMs as shown in Fig. S5. We note that the reason for the decreased localization of the states observed here compared to the specially designed SAMs discussed in ref. S7 is a consequence of (i) the smaller dipoles and corresponding energy shifts of the pyrimidines used here compared to the methylated bipyrimidines in ref. S7 and (ii) the smaller conjugation length of the molecular segments above and below the polar units making a localization of the states energetically more costly.

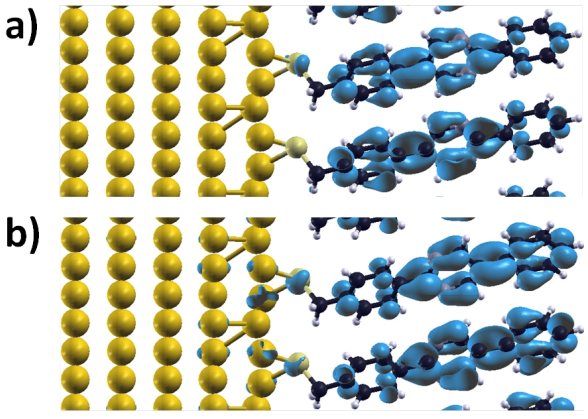

Figure S6: Local densities of states associated with the lowest unoccupied peaks of the PDOS of TP1-down (a)) and TP1-up (b)).

References

(S1) E. A. Weiss, G. K. Kaufman, J. K. Kriebel, Z. Li, R. Schalek and G. M. Whitesides, *Langmuir*, 2007, **23**, 9686–9694.

(S2) D. Fracasso, H. Valkenier, J. C. Hummelen, G. C. Solomon and R. C. Chiechi, *J. Am. Chem. Soc.*, 2011, **133**, 9556–9563.

(S3) T. Abu-Husein, S. Schuster, D. A. Egger, M. Kind, T. Santowski, A. Wiesner, R. Chiechi, E. Zojer, A. Terfort and M. Zharnikov, *Adv. Func. Mater.*, 2015, **25**, 3943–3957.

(S4) G. Kresse and J. Furthmüller, *Phys. Rev. B*, 1996, **54**, 11169–11186.

(S5) J. P. Perdew, K. Burke and M. Ernzerhof, *Phys. Rev. Lett.*, 1996, **77**, 3865–3868.

(S6) F. Rissner, D. A. Egger, A. Natan, T. Körzdörfer, S. Kümmel, L. Kronik and E. Zojer, *J. Am. Chem. Soc.*, 2011, **133**, 18634–18645.

(S7) B. Kretz, D. A. Egger and E. Zojer, *Adv. Sci.*, 2015, **2**, 1400016.